Jeong, H. S., Nara, Y., Obara, Y., Kaneko, K., Stress corrosion index of Kumamoto andesite estimated from two types of testing method.
International Symposium on the Fusion Technology of Geosystem Engineering, Rock Engineering and Geophysical Exploration
Seoul, Korea, Nov. 18-19, 2003

Stress corrosion index of Kumamoto andesite estimated from two types of testing method

Hae-Sik Jeong[1], Yoshitaka Nara[2], Yuzo Obara[3], Katsuhiko Kaneko[2]
[1]Seoul National University, Seoul, Korea, [2]Hokkaido University, Sapporo, Japan
[3]Kumamoto University, Kumamoto, Japan

Abstract: The stress corrosion index of Kumamoto andesite are evaluated by two types of testing method. One is the uniaxial compression test under various water vapor pressures, and the other is the double torsion (DT) test under a constant water vapor pressure. For the uniaxial compression tests, the uniaxial compressive strength increases linearly with decreasing water vapor pressure on the double logarithmic coordinates. As the results, the stress corrosion index obtained is estimated 44. On the other hand, in the DT test, the relaxation (RLX) test and the constant displacement rate (CDR) test were conducted. For the CDR test, as the displacement rate of loading point increases, the crack velocity increases. However, the fracture toughness is constant regardless of the change in displacement rate and the average fracture toughness is evaluated 2.07MN/m$^{3/2}$. For the RLX test, the crack velocity–stress intensity factor curves are smooth and linear. The stress corrosion index estimated from the curves is 37. Comparing stress corrosion indexes in the uniaxial compression test and the DT test, there is no significant difference in these values, and they are considered to be in coincident each other regardless of testing methods. Therefore, it is concluded that stress corrosion is one of material constants of rock.

1. Introduction

Stress corrosion index can be evaluated from DT test (Atkinson, 1979, 1980; Sano and Kudo, 1992; Seto et al., 2000), uniaxial compression test (Sano et al., 1981; Obara et al., 1996a, 1996b; Jeong et al., 2003) and creep test (Schmidtke and Lajtai, 1985; Lockner, 1993). This index has been recognized as a parameter representing the property of rock. Sano et al. (1981) showed that stress corrosion indexes of crystalline silica-rich rocks seemed to have the values around 30. Many researchers have been investigated that the stress corrosion index increases with increasing water vapor pressure (Waza et al., 1980; Swanson, 1984; Lajtai and Schmidtke, 1986). However, there are few experiments with a change in water vapor pressure. Furthermore, there are few reports about the evaluation of stress corrosion index by the different type of experiments, using same kind of rock specimen.

In this paper, the stress corrosion index is evaluated using a kind of rock specimen by two types of testing method. That is, the uniaxial compression tests under various water vapor pressures and the DT test under a constant water vapor pressure are conducted on Kumamoto andesite. The stress corrosion indexes obtained by two types of testing method are compared and examined.

2. Fundamentals of Testing Method

Uniaxial compression test

In case that crack velocity is proportional to water vapor pressure, the power law of crack velocity *da/dt* due to stress corrosion dependence on the tensile stress at a crack tip in brittle materials can be represented to the following equation (Wiederhorn, 1967; Martin, 1972):

$$da/dt = A \cdot p^{n_w} \cdot \sigma^n \cdot a^{\frac{n}{2}} \tag{1}$$

where A is a proportional constant, n_w is the order of the rate-limiting chemical reaction, n is stress corrosion index and a is crack length. Assuming that stress rate $\dot{\sigma}$ is constant in uniaxial compression test and integrating from initial crack length a_0 to critical crack length a_c at time $t = t_c$, the following equation is obtained.

$$\frac{1}{1-n/2}\left(a_c^{1-n/2} - a_0^{1-n/2}\right) = A \cdot p^{n_w} \cdot \dot{\sigma}^n \cdot \frac{t_c^{n+1}}{n+1} \tag{2}$$

Assuming that failure occurs when the stress reaches critical value S_c, t_c becomes

$$t_c = S_c / \dot{\sigma} \propto S_c / \dot{\varepsilon} \quad (3)$$

where $\dot{\varepsilon}$ is strain rate. From eq. (2) and eq. (3), the following relation is obtained.

$$S_c^{n+1} \propto \dot{\varepsilon} / p^{n_w} \quad (4)$$

When n_w is assumed to be equal to unity, n becomes to stress corrosion index. Therefore,

$$\log S_c \propto \frac{1}{n+1} \log\left(\frac{\dot{\varepsilon}}{p}\right) \quad (5)$$

This equation coincides with those suggested by Sano et al. (1981), Kato et al. (1993) and Seto et al. (2000).

Double torsion test

Fig. 1 shows the plot of the logarithm of the stress corrosion crack velocity v against the stress intensity factor K_I. In region I, the relation is linear, and the crack velocity is controlled by the rate of stress corrosion reaction at the crack tip. In region II of plateau, the crack velocity is independent of stress and controlled by the mass transport of corrosive reactants to the crack tip. In region III, crack growth curves are quite steep and K_I is close to critical stress intensity factor, namely fracture toughness. The crack growth in this region is controlled by mechanical rupture and it is relatively insensitive to the chemical environment (Evans and Johnson, 1975; Freiman, 1984).

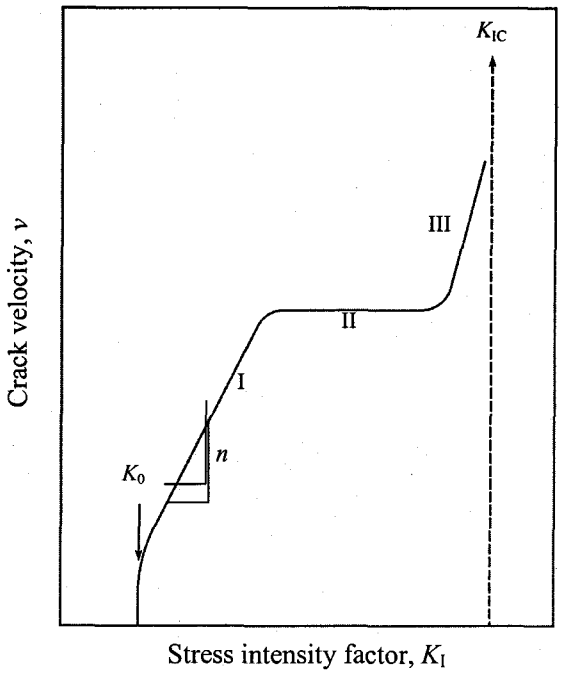

Fig. 1. The variation of stress intensity factor with crac velocity.

The crack velocity against stress intensity factor in region I is represented by the following power law (Martin, 1972; Atkinson, 1980):

$$v = \alpha K_I^n \quad (6)$$

where n is stress corrosion index, and α is a constant. The double torsion (DT) test is one of reliable methods for the investigation of crack growth in region I.

The basic geometry of a DT specimen is illustrated in Fig. 2. The specimen is a thin plate, which is notched and grooved along the length of the specimen to guide a crack. The load is applied to the end of the specimen in torsion by four-point loading. Then the crack is propagated along the guide groove.

Williams and Evans (1973) suggested the method to calculate stress intensity factor K_I and crack velocity *da/dt* in DT test under the condition of a constant displacement as the following equations.

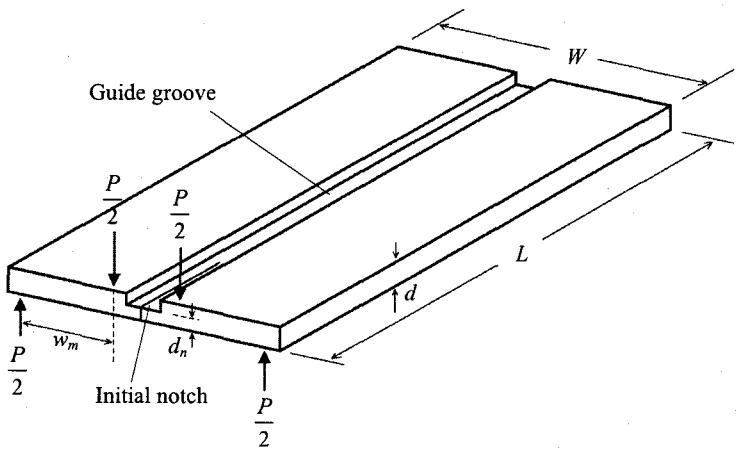

Fig. 2. Schematic view of double torsion test.

$$K_I = Pw_m \left[\frac{3(1+\nu)}{Wd^3 d_n}\right]^{1/2} \tag{7}$$

$$\left(\frac{da}{dt}\right)_{\frac{du}{dt}=const} = \phi \frac{1}{BP_{\max}} \frac{du}{dt} \tag{8}$$

$$\left(\frac{da}{dt}\right)_{u=const} = -\phi \frac{P_i \lambda_i}{BP^2} \frac{dP}{dt} \left(B = \frac{3w_m^{\ 2}}{Wd^3 \mu}\right) \tag{9}$$

where P is applied load, du/dt is the rate of displacement, dP/dt is the rate of load relaxation, P_i and λ_i are the initial values of load and compliance, ν and μ are Poisson's ratio and shear modulus of the material and ϕ is a factor depending on the crack geometry. w_m, W, d and d_n are the same as in Fig. 2. From eq. (7), (8) and (9), stress intensity factor and crack velocity for DT configuration are expressed as a function of applied load, specimen dimensions, Poisson's ratio and Young's modulus. Therefore, DT test has been widely used for the study of subcritical crack growth in the world, because that the configurations of loading system and specimen are simple and that stress intensity factor is independent of crack length (Williams and Evans, 1973).

3. Specimen and Testing Procedures

Specimen

The rock used in uniaxial compression test and DT test is Kumamoto andesite. Because that Kumamoto andesite is isotropic and homogeneous (Obara et al., 1992), The specimen for uniaxial compression test and DT test are made from a cubic block randomly. Kumamoto andesite is porphyritic and consists of plagioclase (about 50%), hornblende and augite (2~3%) as phenocryst and fine-grained groundmass. Kitagishima granite is consists of quartz (34.6%), plagioclase (34.4%), orthoclase (27.7%), biotite (2.2%), chlorite (1.1%) and other minor minerals.

As the dimensions of the specimen, the diameter and length of the specimen are 35mm and 70mm in the uniaxial compression test. Two kinds of specimen are used in the DT test: one is without guide groove for the CDR test, the other is with guide groove for the RLX test. Both specimens have an initial notch. The dimensions of the former are the width W, length L and thickness d of the specimen are 45, 130 and 2mm respectively. The dimensions of the latter are $W = 45$, $L = 130$ and $d = 3$mm. The guide groove with a depth of 1mm is cut at the central part of the specimen along its length. The length of the initial notch is 25mm. The schematic view of the specimen having guide groove is shown in Fig. 3.

In order to achieve complete dry condition of the rock specimens, these were dried in the electric drier oven at constant temperature 197°C and kept in a desiccator after drying.

Uniaxial compression test

A vacuum chamber was made to control the surrounding environment of rock as shown in Fig. 4. The chamber, which is made of SUS304, has six ports and a valve to inject gases. In these ports, two ports are used to lead the output from strain gauges pasted to the specimen surface. Another two ports are to measure the vapor pressure in the chamber by two pressure gauges, namely a pirani pressure gauge which measurement range is 10^5 to 10^{-1}Pa and

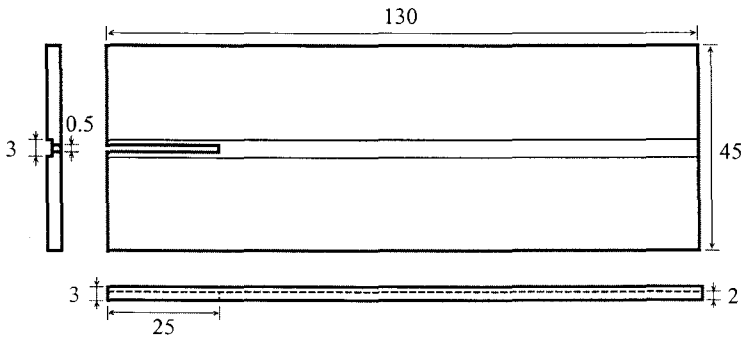

Fig. 3. Dimensions of DT specimen used in this research (unit : mm).

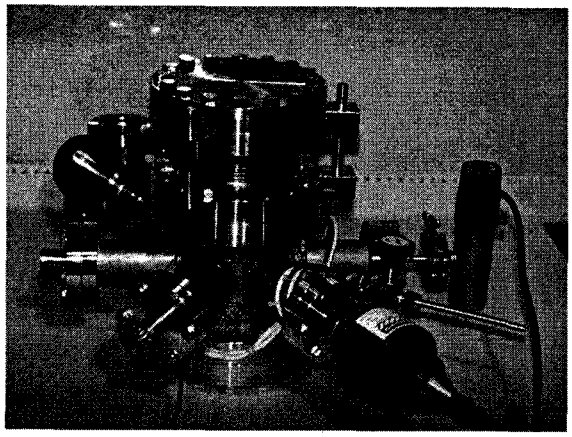

Fig. 4. Picture of a vacuum chamber.

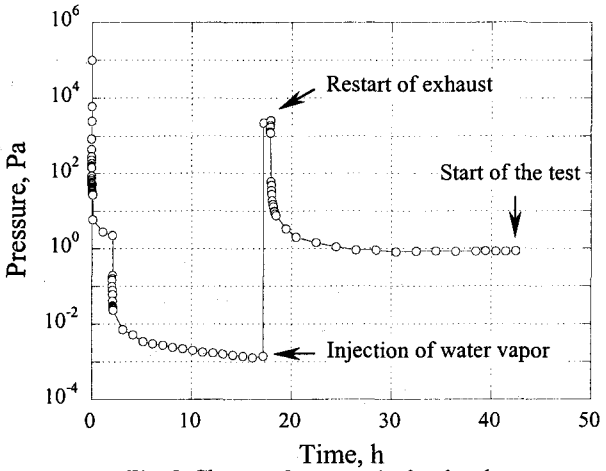

Fig. 5. Change of pressure in the chamber.

a penning pressure gauge which measurement range is 10^0 to 10^{-6}Pa. One port is the window for observing inside of the chamber and the last port with a valve is used as the evacuation of the air in the chamber by vacuum pumps.

Two pumps, a rotary vacuum pump and turbo molecular vacuum pump, are used to change the environment in the chamber to water vapor environment. These pumps are connected to the evacuation valve of the chamber with flexible tube.

Fig. 5 shows the change of the pressure in the chamber during test. At first, after the air in the chamber was evacuated by using two vacuum pumps until the pressure of about 10^{-3}Pa, then the distilled water was injected through the injection valve to a pressure of about 10^3Pa. As the result, it is considered that the pressure in the chamber becomes the saturated water vapor pressure at room temperature and that the chamber is filled with only water vapor. Then the water vapor in the chamber was exhausted again. After the required water vapor pressure was maintained for about 24 hours, the uniaxial compression test was performed.

500kN servo-controlled testing machine was used for the test. The applied load is controlled by a constant strain rate.

Double torsion test

Fig. 6 shows an apparatus for DT test. A specimen is supported by six steel ball bearings (4mm in diameter) and the load generated by the electric cylinder is applied on the end of the specimen through the four ball bearings. It is possible that torsional moment is subjected to the specimen and a tension crack is propagated along the guide groove of the specimen. The moment arm w_m, which is the distance between two ball bearings of the upper and lower plate, is 18mm as shown in Fig. 2. The state of induced crack is observed from a digital microscope (×175) under the loading apparatus. The applied load is measured by load cell. The displacements of the loading points are monitored by two displacement transducers.

In the DT test, the relaxation (RLX) test and constant displacement rate (CDR) test are conducted. The procedures of each test include the pre-cracking and the constant displacement rate test in CDR test and the pre-cracking, the measurement of initial compliance and the load relaxation test in RLX test.

Prior to the CDR or RLX test, the pre-cracking of the DT specimen is necessary to achieve a 'natural crack'. The natural crack is produced from the end of the notch. This technique is followed to Pletka et al. (1979). The specimen is loaded at a slow speed, and then the displacement is fixed for a while so that a constant load is maintained on the specimen. Then load is reduced. After that, the load is increased again and the displacement is fixed. This process is

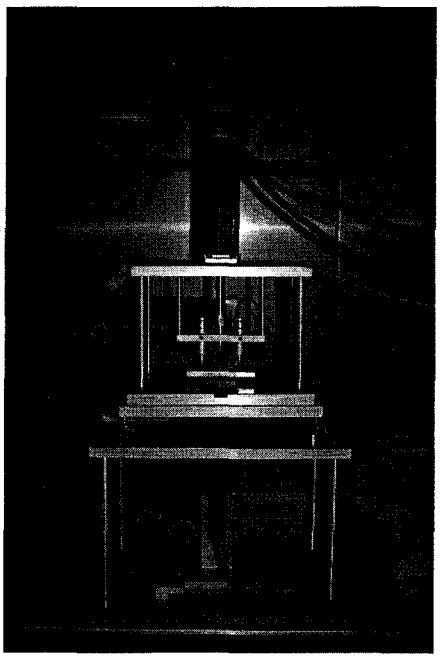

Fig. 6. Photograph of apparatus for DT test.

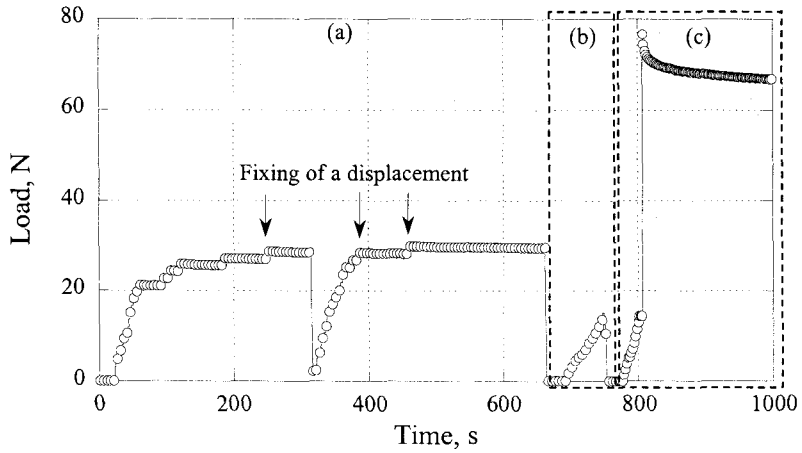

Fig. 7. Procedures of the RLX test. (a) precracking, (b) measurement of initial compliance, (c) load relaxation test.

repeated until a natural crack is initiated. In case that the crack is initiated, the load decreases in spite of the constant displacement. After this behavior is confirmed, the load is removed rapidly. The state of natural crack is observed by the digital microscope during repeat of loading. The load for the pre-cracking is about 25N in the CDR test and 30N in RLX test.

At first, the CDR test is conducted to obtain the fracture toughness K_{IC}, using pre-cracked specimen. Bruce and Koepke (1977) suggested that K_{IC} must be measured on pre-cracked specimens during loading at crosshead speeds high enough to initiate fast catastrophic crack growth. This test followed his method to measure K_{IC}. In order to remove the influence of impact load to the specimen and apply load on the loading point accurately, the specimen is loaded to about 7N initially. Then the load is applied with a constant displacement rate until the specimen failures. The load shows the peak value P_{max}. The fracture toughness and the crack velocity are calculated by this value, according to eq. (7) and (8).

Secondly, the RLX test is conducted to obtain the relation between crack velocity and stress intensity factor. The DT specimen with a guide groove is installed on the ball bearing on the lower plate and the guide groove is set upward. At the beginning of the test, the natural crack is produced in the same manner of the CDR test. After that, the initial compliance of a pre-cracked specimen is necessary to be evaluated before the RLX test. The specimen is loaded up to about 16N at a slow speed. In this time, the load P and the vertical displacement u at a time is measured. From the relation of the two variables, the initial compliance $\lambda_i=du/dP$ can be obtained. Then the RLX test is conducted subsequently.

The change in load and displacement during the RLX test is shown in Fig. 7. After applying load to about 15N initially in the same manner of the CDR test, the specimen is loaded rapidly until displacement is arrived to the set-up value so that no significant crack extension occurs prior to the relaxation. When a required load P_i is reached, the displacement is fixed. In this time, the load is relaxed as the crack propagates. Monitoring the load as a function of time during about 2 hours, the stress intensity factor and the crack velocity are evaluated according to eq. (7) and (9). In the test, the load P_i was determined as the value corresponding to the stress intensity factor of 90% of the fracture toughness obtained by the CDR test.

A controllable box is used in order to maintain temperature and relative humidity constant during the test. The box is set around the loading part including specimen. The CDR test or RLX test are conducted after temperature and relative humidity in the box are made to be constant.

4. Experimental Results

Uniaxial compression test

The conditions and results of uniaxial compression test for Kumamoto andesite are summarized in Table 1. The strain rate is controlled to about 2.0×10^{-5}/s and the water vapor pressure in the chamber is between 4.2×10^{-3} and 1.2×10^{3}Pa. The typical stress-strain curves are shown in Fig. 8. It is shown that uniaxial compressive strength is higher with decreasing water vapor pressure. The axial strain curves show linear behavior from the start but the slopes of the curves become non-linear as approaching to failure.

Table 1. Conditions and results of uniaxial compression test.

No.	Strain rate (10^{-6}/s)	Water vapor pressure (Pa)	Strength (MPa)	Young's modulus (GPa)	Poisson's ratio
1	1.98	1.2×10^{3}	128.3	27.2	0.21
2	1.88	2.0×10^{2}	153.0	29.3	0.22
3	2.41	9.0×10^{1}	160.4	29.4	0.22
4	1.75	3.6×10^{0}	174.6	35.8	0.24
5	2.33	9.0×10^{-1}	177.2	35.1	0.23
6	2.74	6.0×10^{-1}	174.2	32.2	0.23
7	2.50	1.0×10^{-1}	180.0	29.2	0.21
8	2.71	1.5×10^{-2}	179.5	30.4	0.22
9	2.66	1.0×10^{-2}	175.1	31.9	0.24
10	2.54	4.2×10^{-3}	190.2	34.9	0.24

Young's modulus and Poisson's ratio measured at 50% of the strength were measured as shown in Table 1. It is considered that Young's modulus and Poisson's ratio are independent of water vapor pressure. Its average values are 31.5GPa and 0.23 respectively.

The relation between the uniaxial compressive strength S_c and the ratio of strain rate to water vapor pressure $\dot{\varepsilon}/p$ is shown in Fig. 9. The plots are somewhat scattered but the strength S_c increases as the ratio $\dot{\varepsilon}/p$ increases. The linear regression equation of the plots is obtained as follows:

$$\log S_c = N_c \log(\dot{\varepsilon}/p) + \log S_{c0} \tag{10}$$

where S_{c0} is the uniaxial compressive strength when p = 1Pa and N_c is the slope of the line. Compared eq. (10) with eq. (5), N_c is coincident with the term $1/(n+1)$. The stress corrosion index obtained from the uniaxial compression test with a change in water vapor can be estimated 44.

Double torsion test

In the CDR tests, the displacement rate *du/dt* is adopted to 0.10 and 0.23mm/s. The maximum load is evaluated with consideration of the weight of the upper plate placed on the specimen. These are constant and the average is 46.6N independent of the displacement rate.

The fracture toughness and crack velocity were calculated by eq. (7) and (8). Young's modulus and Poisson's ratio were used from the results of the uniaxial compression test. As the displacement rate increases, the crack velocity increases. However, K_{IC} is constant and independent of the displacement rate. The average of fracture toughness

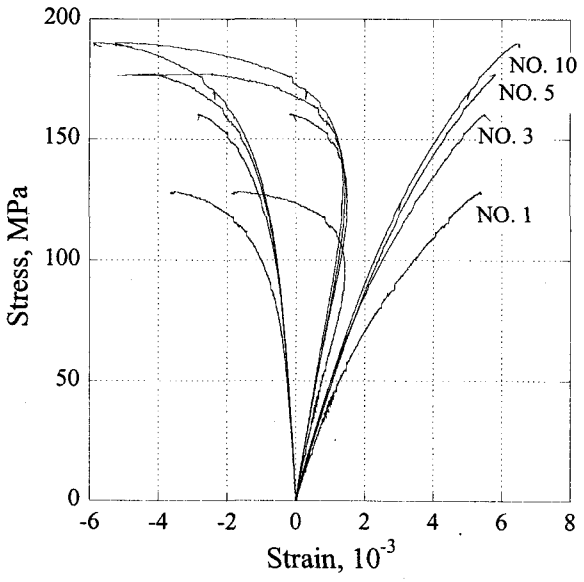

Fig. 8. Stress-strain curves.

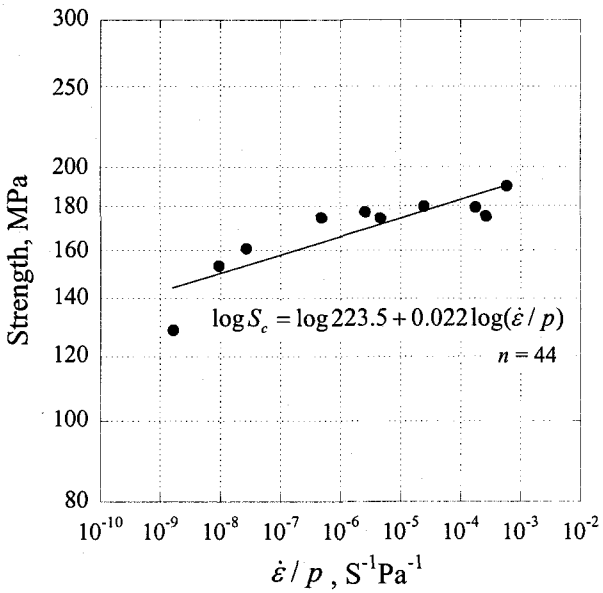

Fig. 9. Relation between the strength and water vapor pressure

in each specimen was 2.07MN/m$^{3/2}$. For the calculation of the crack velocity, the factor ϕ in eq. (8) is set unity for the convenience of calculation in this study.

Initial compliance λ_i of the pre-cracked specimen was measured before the RLX test in order to estimate the crack velocity. The initial compliance was estimated from the slope of the regression curve in a region of the load from 7N to 15N to obtain the accurate data. The initial compliance was obtained 2.11×10^{-6}m/N in average.

In the RLX tests, the required load was set about 80N and the displacement was fixed. Then the rate of load relaxation dP/dt is calculated from the load relaxation curve, as shown in Fig. 7. The determination of dP/dt to calculate crack velocity followed the method suggested by Pletka et al. (1979). The data is obtained by measuring the time for a specific load decrement. Because that the minimum output from the load cell used in this study is 0.04N, the slope of a least squares fit of the data for the load decrement of 0.2N for its accuracy was adopted as the rate of load relaxation at that load. Then the stress intensity factor and the crack velocity based on eq. (7) and (9) are calculated using a program. The factor ϕ in eq. (9) is set unity for the convenience of calculation in the same manner of the CDR test.

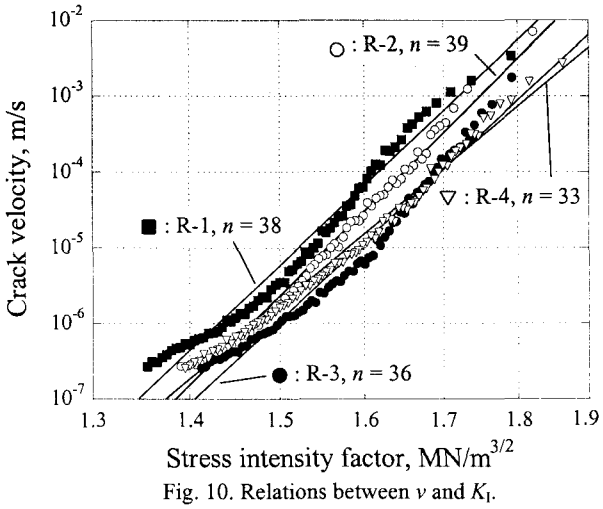

Fig. 10. Relations between v and K_I.

The relations between crack velocity and stress intensity factor for 4 specimens are shown in Fig. 10. All of the data are plotted linearly. This relation can be expressed by eq. (6). The slope of the linear relation is correspondence to stress corrosion index in double logarithmic coordinates. This value is almost the same in all 4 specimens. The average value of stress corrosion index for DT test is 37. The conditions and results for RLX test are summarized in Table 2.

The stress corrosion index of Kumamoto andesite was estimated in this research as follows: n is 44 in case of uniaxial compression test with a change in water vapor and 37 in case of DT tests under a constant water vapor pressure. These values were obtained, using specimens formed from one rock block. Stress corrosion indexes obtained from uniaxial compression test and Brazilian test under various loading rates are 31 and 34 respectively, using specimens get from other blocks of Kumamoto andesite (Jeong, 2003). These values are similar regardless of experimental method. Stress corrosion index for Kumamoto andesite is 40 in average. Putting these results together it is concluded that stress corrosion index of rock is one of material constants of rock.

5. Conclusions

In order to investigate the stress corrosion index by the different methods and estimate the long-term strength by stress corrosion, uniaxial compression test and DT test are conducted in water vapor environment using Kumamoto andesite. The obtained results are as follows:

1. For uniaxial compression tests, the uniaxial compressive strength increases linearly as water vapor pressure decreases on the double logarithmic coordinates and stress corrosion index obtained are 44.

2. For CDR tests, as the displacement rate of the loading point du/dt increases, the crack velocity increases. However, the fracture toughness is constant regardless of the du/dt and the average fracture toughness is 2.07MN/m$^{3/2}$.

Table 2. Conditions and results of relaxation test.

No.	T (°C)	R.H. (%)	p (Pa)	λ_i (10^{-6}m/N)	Stress corrosion index n
R-1	10.9	43	561	2.08	38
R-2	10.9	44	574	2.07	39
R-3	10.9	44	574	2.13	36
R-4	10.9	43	561	2.13	33
Average	10.9	44	566	2.10	37

3. For RLX tests, the resulting crack velocity–stress intensity factor curves are smooth and very nearly linear. And average stress corrosion index obtained by least squares method is 37.

4. Comparing stress corrosion indexes for uniaxial compression tests and DT tests, it is considered that they are in coincident regardless of experimental methods. Putting these results together, it is concluded that stress corrosion index of rock is one of material constants of rock.

References

Atkinson, B. K., 1979, Fracture toughness of Tennessee sandstone and Carrara marble using the double torsion testing method, Int. J. Rock Mech. Min. Sci. Geomech. Abstr., 16, 49-53.

Atkinson, B. K., 1980, Stress corrosion and the rate-dependent tensile failure of a fine-grained quartz rock, Tectonophysics, 65, 281-290.

Bruce J. G., Koepke, B. G., 1977, Evaluation of K_{IC} by the double-torsion technique, J. Am. Ceram. Soc., 60, 284-285.

Evans, A. G., Johnson, H., 1975, The fracture stress and its dependence on slow crack growth, J. Mater. Sci., 10, 214-222.

Freiman, S. W., 1984, Effects of chemical environments on slow crack growth in glasses and ceramics, J. Geophys. Res., 89, 4072-4076.

Jeong, H. S., 2003, Fundamental study on the mechanical behavior of rock under various surrounding environments, Ph. D. Dissertation, Kumamoto University.

Jeong, H. S., Obara, Y., Sugawara, K., 2003, The strength of rock under water vapor pressure, Shigen-to-Sozai, 119 9-16 (in Japanese).

Kato, N., Yamamoto, K., Yamamoto, H., Hirasawa, T., 1993, A stress-corrosion model for strain-rate dependence of the frictional strength of rocks, Int. J. Rock Mech. Min. Sci. Geomech. Abstr., 30, 551-554.

Lajtai, E. Z., Schmidtke, R. H., 1996, Delayed failure in rock loaded in uniaxial compression, Rock Mech. Rock Eng., 19, 11-25.

Lockner, D., 1993, Room temperature creep in saturated granite, J. Geophys. Res., 98, 475-487.

Martin, R. J., III, 1972, Time-dependent crack growth in quartz and its application to the creep of rocks, J. Geophys Res., 77, 1406-1419.

Obara, Y., Hirokawa, H., Sugawara, K., 1996a, The strength of rocks under lower water vapor pressure, Proc. 1st Korea-Japan Joint Symposium on Rock Engineering, Seoul, Korea, 109-114.

Obara, Y., Sakaguchi, K., Nakayama, T., Sugawara, K., 1992, Anisotropy effect on fracture toughness of rock, Proc. ISRM Symposium : Eurock '92, Telford, T., London, 7-12.

Obara, Y., Sugawara, K., Tokashiki, N., 1996b, Influence of water vapor pressure on strength of rocks under uniaxial compression, Proc. 2nd North American Rock Mechanics Symposium: NARMS '96, Balkema, A. A., Rotterdam, 1337-1342.

Pletka, B. J., Fuller, E. R., Jr., Koepke, B. G., 1979, An evaluation of double-torsion testing – experimental, ASTM STP, 678, 19-37.

Sano, O., Kudo, Y., 1992, Relation of fracture resistance to fabric for granitic rocks, Pure and Applied Geophysics, 138, 657-677.

Sano, O. Ito, I., Terada, M., 1981, Influence of strain rate on dilatancy and strength of Oshima granite under uniaxial compression, J. Geophys. Res., 86, 9299-9311.

Schmidtke, R. H., Lajtai, E. Z., 1985, The long-term strength of Lac du Bonnet granite, Int. J. Rock Mech. Min. Sci Geomech. Abstr., 22, 461-465.

Seto, M., Utagawa, M., Jung, W. J., 2000, Subcritical crack growth and rate dependent tensile failure of sandstones, Sigen-to-Sozai, 116, 630-635 (in Japanese).

Swanson, 1984, Subcritical crack growth and other time- and environmental-dependent behavior in crustal rocks, J. Geophys. Res., 89, 4137-4152.

Waza, T., Kurita, K., Mizutani, H., 1980, The effect of water on the subcritical crack growth in silicate rocks, Tectonophysics, 67, 25-34.

Williams, D. P., Evans, A. G., 1973, A simple method for studying slow crack growth, J. Test. Eval., 1, 264-270.

Wiederhorn, S. M., 1967, Influence of water vapor on crack propagation in soda-lime glass, J. Am. Ceram. Soc., 50 407-414.